

# Preparation and mechanical properties of Ni-Cr-Al alloy by EB-PVD<sup>①</sup>

GUAN Chunlong(关春龙), HE Xiaodong(赫晓东), LI Yao(李垚)  
(Center for Composite Materials, Harbin Institute of Technology,  
Harbin 150001, China)

**Abstract:** Ni-Cr-Al alloy was deposited by electron beam-physical vapor deposition (EB-PVD) method. The microstructure was investigated on as-deposited and long-term aged alloy. The results indicate that grain on surface of as-deposited alloy is about 185 nm in size, and a laminated structure in cross-section is observed. However, after aging for 16 and 120 h at 760 °C, the laminated structure is dissolved, and the individual grain can be seen clearly. Columnar crystals form on the evaporation side, and equiaxed grains form on the substrate side. The major precipitate is  $\gamma$  phase after prolonged aging at 760 °C. Mechanical properties of the Ni-Cr-Al alloy were also studied. The results show that the fracture of as-deposited alloy has mixed type at room temperature, and intergranular fracture among columnar crystals is observed. Compared to that of as-deposited alloy, fracture of alloy after aging for 16 and 120 h at 760 °C appears to involve ductile fracture with dimples.

**Key words:** Ni-Cr-Al alloy; physical vapor deposition; microstructure; mechanical properties; columnar crystal

**CLC number:** TG 146.2

**Document code:** A

## 1 INTRODUCTION

Ni-based superalloys are presently used as gas turbine components in power plants and in aircraft engines<sup>[1-3]</sup>. Since 1970s, Al has been added to Ni-Cr alloy for producing the hard elastic alloys used as wear resistant components in instruments<sup>[4]</sup>. This is an important development in Ni-Cr alloy. With the increasing demands for the alloys with high hardness and toughness, Ni-Cr-Al alloys are designed to meet the requirement. Due to the addition of Ce element, forgeable temperature was decreased, and grains were refined, and the inclusions were removed<sup>[5]</sup>.

LIU<sup>[6, 7]</sup> have performed extensive research on the behavior of Ni-Cr-Al hard elastic alloy. Their results indicated that a number of Cr ( $\alpha$ )-rich phase were found around  $\gamma$  phase with tiny grains and dispersed distribution when aged at 550 °C for 5 h. But Cr ( $\alpha$ )-rich phase was not observed in this work. Ni-Cr-Al alloys were usually produced by vacuum melting and cast process. But reports about Ni-Cr-Al alloy prepared by electron beam-physical vapor deposition (EB-PVD), which is often used to produce the thermal barrier coatings (TBCs)<sup>[8-11]</sup>, are few.

Electron beam-physical vapor deposition (EB-PVD) technology is a potential technique for producing near theoretical density and oxide-free condensates<sup>[12-14]</sup>. Due to its high deposition rate, easy

control for chemical constitution and pollution-free to environment, Ni-Cr-Al alloy with 0.5 mm in thickness was deposited by EB-PVD process. In this work, microstructure and mechanical properties of an EB-PVD formed Ni-Cr-Al alloy are studied.

## 2 EXPERIMENTAL

Ni-Cr-Al alloy was prepared by EB-PVD. The chemical composition of Ni-Cr-Al ingots is Ni-22Cr-5Al-0.6Y (mass fraction, %). The process of the preparation of deposited alloy by EB-PVD is shown in Fig. 1.

Before the alloy was fabricated, the resistance adhesive layer with about 15  $\mu$ m in thickness

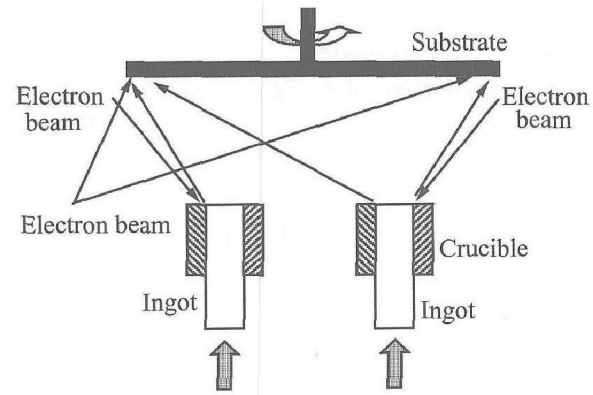


**Fig. 1** Schematic diagram of EB-PVD process of Ni-Cr-Al alloy

① **Foundation item:** Project(2002AA763020) supported by the Hi-tech Research and Development Program of China

**Received date:** 2004-11-15; **Accepted date:** 2005-01-18

**Correspondence:** GUAN Chunlong, PhD; Tel: +86-451-89678120; E-mail: gel\_hit@163.com

should be deposited to prevent bonding between substrate and condensate. The Ni-Cr-Al ingots of 100 mm in diameter and 200 mm in length were filled in a water-cooled crucible. A stainless steel disk substrate of 800 mm in diameter and 20 mm in thickness was mounted on the vertical axis. The substrate was heated by electron beam and the temperature was kept at 900 °C. The degree of vacuum was  $5 \times 10^{-4}$  Pa during evaporation. Thickness of the alloy could be controlled by adjusting the beam current, the upward speed of the ingots and rotation speed of the substrate. The rotation speed of the substrate was 36 r/min. The deposition rate of the alloy was 1.8  $\mu\text{m}/\text{min}$ . In this work, the Ni-Cr-Al alloy with 0.5 mm in thickness was prepared by EB-PVD, and aged at 760 °C for 16 and 120 h.

The SEM samples of the tested alloy were ground to 13  $\mu\text{m}$  and mechanically polished, then etched with a solution of HCl, HNO<sub>3</sub>, HF and H<sub>2</sub>O. The TEM samples were mechanically thinned down to 50–100  $\mu\text{m}$  in thickness, and electropolished with a solution of 7% perchloric acid and ethanol at –30–20 °C by a double jet electropolisher. Tensile tests at room temperature were carried out by Instron 5500.

### 3 RESULTS AND DISCUSSION

#### 3.1 Microstructures of tested alloy

Microstructures in the deposited condition are shown in Fig. 2. Based on the AFM and TEM images given in Fig. 2, grain size on the surface of vapor-deposited alloy is in the range of 70–255 nm, and average size is about 185 nm. However, average size of the alloy annealed at 760 °C for 16 h is about 4  $\mu\text{m}$  (Fig. 3(a)). Convergent beam diffraction shows that the as-deposited alloy has single phase and a laminated structure is observed in the cross-section of as-deposited alloy, as shown in Fig. 2(b). After annealing at 760 °C for 16 h, the laminated structure dissolves and the individual grain can be seen clearly. Schulz et al.<sup>[15]</sup> EB-PVD-deposited a ceria-stabilized TBC by one-source and two-source jumping evaporation. A lamellar structure was also observed in the cross-section, which can be attributed to the difference in vapor pressure of ceria and zirconia. Therefore, it can be concluded that in this study the laminated structure in cross-section can be contributed to the difference in vapor pressure of nickel, chromium and aluminum.

Columnar crystals form on the evaporation side, and equiaxed grains form on the substrate side (Fig. 3(b)). Formation of columnar crystals attributes to the substrate with lower temperature, the higher evaporation rate of alloys and the sub-

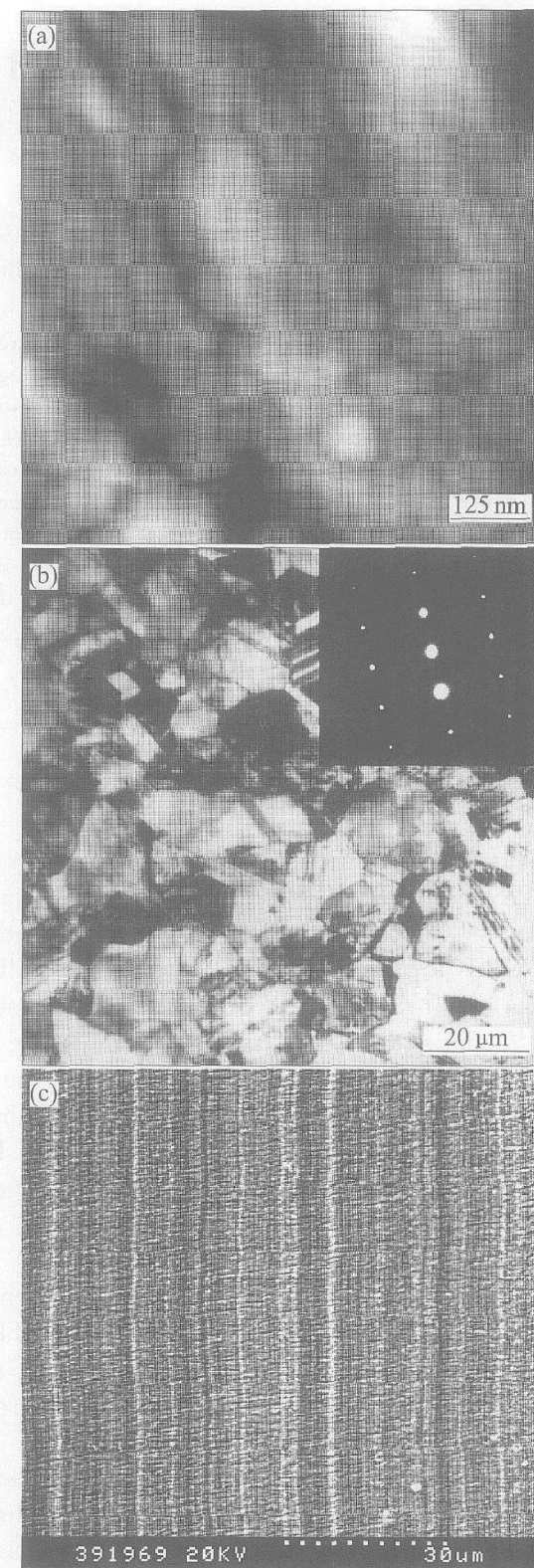
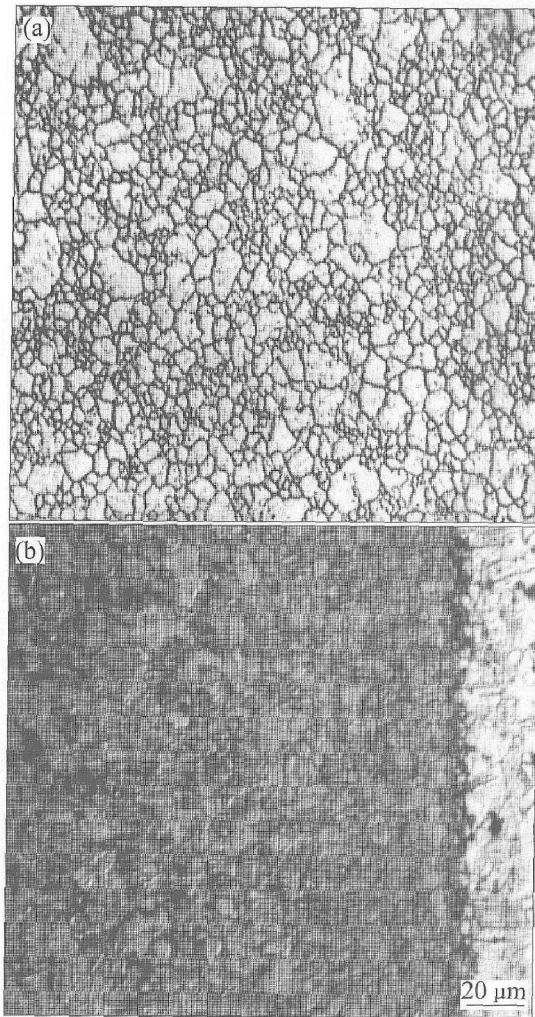


Fig. 2 Microstructure of as-deposited Ni-Cr-Al alloy

- (a) —Surface morphology;
- (b) —TEM image and corresponding diffraction pattern;
- (c) —Cross-sectional morphology

strate with higher degree of coarseness. The surface of substrate has some degree of coarseness, namely some positions can protrude. When vapor atoms touch these positions, preferential nucleation will occur. Furthermore, the substrate temperature and the rate of migration of deposited

atoms are lower. In addition, due to the higher evaporation rate of alloys, the atoms deposited to the substrate will grow quickly along certain direction. As a result, the microstructure of as-deposited alloy is columnar crystals. The major precipitates are  $\gamma'$  phase during prolonged aging at 760 °C. Morphologies of alloy  $\gamma'$  phase in alloy aged at 760 °C for 16 and 120 h are shown in Fig. 4. With an increase in aging time,  $\gamma'$  precipitates grow rapidly. The average size of  $\gamma'$  particles is about 30 and 45 nm respectively.



**Fig. 3** Microstructures of Ni-Cr-Al alloy annealed for 16 h  
(a) —Surface; (b) —Cross-section

### 3.2 Mechanical properties of tested alloy

The SEM fractographs of the tensile samples as-deposited and aged at 760 °C for 16 and 120 h are given in Fig. 5. Fractographs of the as-deposited alloy show that a typical brittle fracture takes place along boundaries of columnar crystals formed in the substrate side (zone A in Fig. 5(a)). This contributes to the weak boundaries among columnar crystals. As shown in zone B in Fig. 5(a), though the equiaxed dimples with little depth are dominant in this region, and some pores are observed. Furthermore, there are no tearing ribs. Therefore,

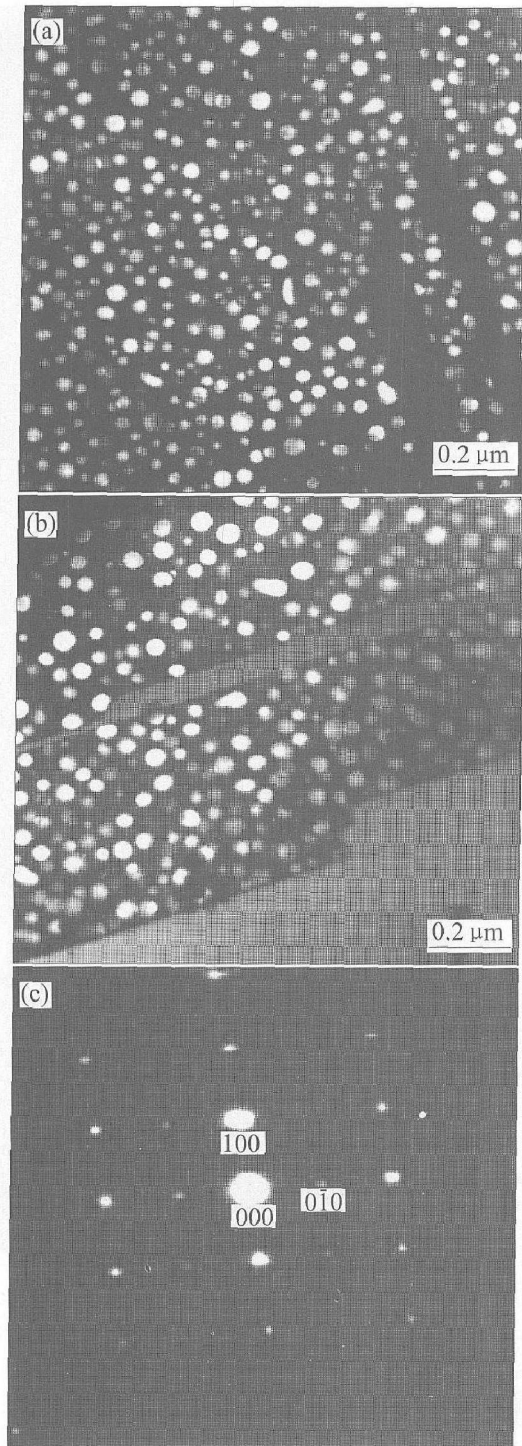


**Fig. 4** TEM micrographs of  $\gamma'$  phase in alloy aged at 760 °C for different time  
(a) —16 h; (b) —120 h;  
(c) —Superlattice pattern from second-phase particle in (a)

elongation value is less than 1%. With increasing aging time, a brittle-to-ductile transition occurs. The fractographs of samples aged at 760 °C for 16 and 120 h indicate an obvious ductile fracture with a lot of dimples, and elongation values increase to more than 10%.

The tensile stress-strain behavior of as-deposited and annealed specimens is shown in Fig. 6. The room temperature tensile strength of EB-PVD processed alloy decreases from 1625 MPa in as-

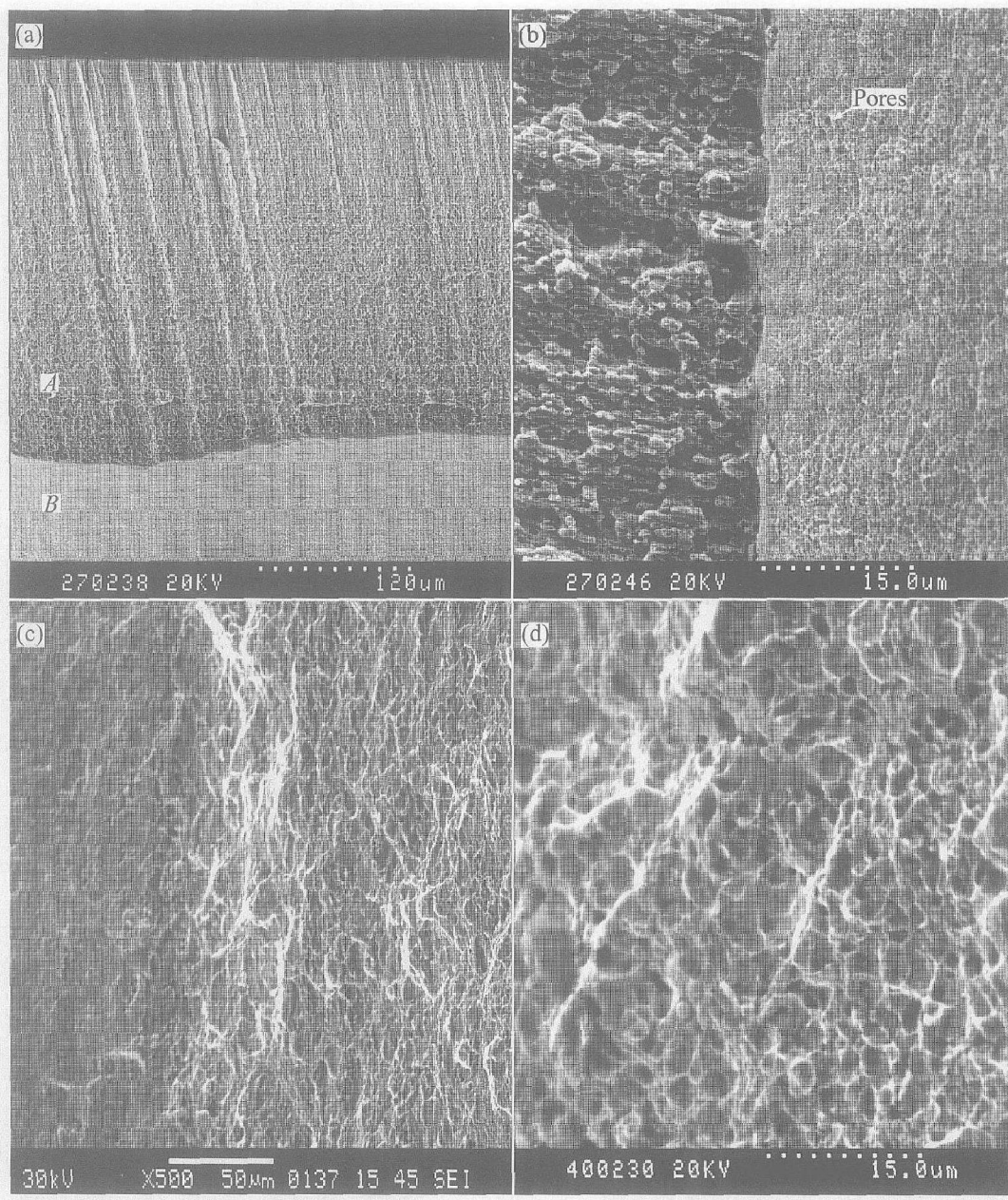


**Fig. 5** Fractographs of as-deposited and annealed Ni-Cr-Al alloy

(a) —As-deposited; (b) —Magnified photograph of (a); (c) —760 °C, 16 h; (d) —760 °C, 120 h

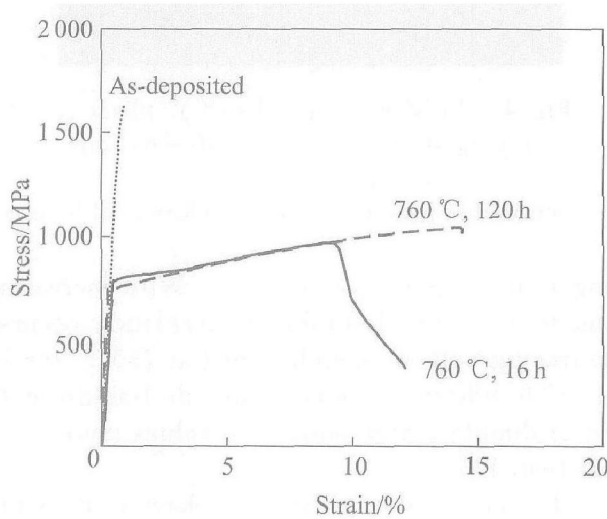


**Fig. 6** Stress—strain behavior of as-deposited and annealed EB-PVD deposits

deposited condition to 831 MPa after annealing at 760 °C for 120 h. Yield strengths of the EB-PVD processed deposits are measured to be 791.8 and 757.3 MPa after annealing for 16 and 120 h at 760 °C, respectively. It can also be noted from Fig. 6 that no yielding is observed in the as-deposited alloy. The as-deposited material shows no sign of plastic deformation whereas annealed material shows a ductile behavior. The mechanical properties of EB-PVD formed Ni-Cr-Al alloy in this study are similar to those of Ni<sub>3</sub>Al materials deposited using vacuum plasma spraying by Tiwari and his co-workers<sup>[16]</sup>.

#### 4 CONCLUSIONS

This study illustrates the potential of producing Ni-Cr-Al alloy sheet with perfect mechanical

properties by EB-PVD. Ni<sub>3</sub>Cr<sub>1</sub>Al alloy with average grain size of 185 nm is deposited using EB-PVD, and a laminated structure in cross-section is observed. After aging for 16 and 120 h at 760 °C, grain on surface grows, and the laminated structure disappears. The major precipitates are  $\gamma$  phase during prolonged aging at 760 °C, and  $\gamma$  phase size increases with aging time. Fractographs of vapor-deposited alloy show that the fracture is mixed type. Brittle fracture takes place along boundaries of columnar crystals formed on substrate side. However, the equiaxed dimples are dominant on the evaporation side. As-deposited alloy has relatively low ductility and no sign of plastic deformation, whereas the annealed alloys show a ductile behavior and higher ductility.

## REFERENCES

[1] ZHAO Shuang-qun, XIE Xishan, Gaylord D, et al. Microstructural stability and mechanical properties of a new nickel-based superalloy [J]. Mater Sci Eng, 2003, A355(1/2): 96 - 105.

[2] Seyed A S, Said N, Roderick I L. Study of microstructure and mechanical properties of high performance Ni-based superalloy GTD-111 [J]. Mater Sci Eng, 2002, A325(1/2): 484 - 489.

[3] CHEN Guofeng, LOU Hanxi. Predicting the oxide formation of Ni<sub>3</sub>Cr<sub>1</sub>Al alloys with nanosized grain [J]. Materials Letters, 2000, 45(9): 286 - 291.

[4] Kniazepa G G. Research of machine properties [J]. Metallurgizdat, 1971, 78(5): 134 - 139.

[5] LI Juntao. Study on Cr<sub>40</sub>Ni<sub>55</sub>Al<sub>3</sub> pivot alloys [J]. Instrument Material, 1978, 4(2): 92 - 98. (in Chinese)

[6] LIU Guilan, ZOU Yuchao. Effect of temperature on structures and properties of Ni<sub>3</sub>Cr<sub>1</sub>Al hard elastic alloys [J]. Journal of Northeastern University, 1994, 15(4): 399 - 402. (in Chinese)

[7] LIU Guilan, ZENG Guiyi. Ageing effect on structures and properties of Ni<sub>3</sub>Cr<sub>1</sub>Al-Ce hard elastic alloys [J]. Journal of Northeastern University, 1995, 16(2): 194 - 197. (in Chinese)

[8] Movchen M, Rudoy Y. Composition, structure and properties of gradient thermal barrier coatings produced by EB-PVD [J]. Materials and Design Materials and Design, 1998, 5/6(19): 253 - 258.

[9] Schulz U, Fritscher K, Komnik Y F, et al. Thermocyclic behaviour of microstructurally modified EB-PVD thermal barrier coatings [J]. Mat Sci Forum, 1997, 251/254(5): 957 - 964.

[10] GUO Hongbo, XU Huibin, BI Xiaofang, et al. Preparation of Al<sub>2</sub>O<sub>3</sub>-YSZ composite coating by EB-PVD [J]. Mater Sci Eng, 2002, A325(1/2): 389 - 393.

[11] Saruhan B, Francois P, Fritscher K, et al. EB-PVD processing of pyrochlore-structured La<sub>2</sub>Zr<sub>2</sub>O<sub>7</sub>-based TBCs [J]. Mater Sci Eng, 2004, A182(2/3): 175 - 183.

[12] Movchen B A. EB-PVD technology in the gas turbine industry: present and future [J]. JOM, 1996, 46(11): 40 - 45.

[13] GUAN Chunlong, LI Yao, HE Xiaodong. EB-PVD technology and its application status [J]. Aeronautical Manufacturing Technology, 2003, 46(11): 35 - 37.

[14] BI Xiaofang, WANG Jiajia, LAN Weihua, et al. Concentration dependence of microstructure and soft magnetic properties in the Fe<sub>3</sub>Si<sub>2</sub>ZrO<sub>2</sub> granular films [J]. Journal of Magnetism and Magnetic Materials, 2004, 281(2/3): 290 - 294.

[15] Schulz U, Fritscher K, Leyens C. Two-source jumping beam evaporation for advanced EB-PVD TBC systems [J]. Surface and Coatings Technology, 2000, 133/134(11): 40 - 48.

[16] Tiwari R, Sampath S, Gudmundsson B, et al. Microstructure and tensile properties of L12-type Ni<sub>3</sub>Cr<sub>1</sub>Al alloy prepared by vacuum plasma spray forming [J]. Scr Metall Mater, 1995, 33(7): 1159 - 1162.

(Edited by YANG Bing)